

Article

Valorization of *Prosopis juliflora* Woody Biomass in Northeast Brazilian through Dry Torrefaction

José Airton de Mattos Carneiro-Junior ¹, Giulyane Felix de Oliveira ², Carine Tondo Alves ³,
Heloyza Martins Carvalho Andrade ^{2,4}, Silvio Alexandre Beisl Vieira de Melo ^{4,5},
and Ednildo Andrade Torres ^{4,5,*}

¹ Department of Biofuels, Federal Institute of Education, Science and Technology of Bahia, Irecê-BA 44900-000, Brazil; airton@ifba.edu.br

² Department of Inorganic Chemistry, Federal University of Bahia, Salvador-BA 40170-115, Brazil; giulyanefelix@hotmail.com (G.F.d.O.); handrade@ufba.br (H.M.C.A.)

³ Department of Energy Engineering, Federal University of the Reconcavo of Bahia, Feira de Santana-BA 44085-132, Brazil; carine.alves@ufrb.edu.br

⁴ Interdisciplinary Center in Energy and Environment, Federal University of Bahia, Salvador-BA 40170-115, Brazil; sabvm@ufba.br

⁵ Industrial Engineering Program, Federal University of Bahia, Salvador-BA 40210-630, Brazil

* Correspondence: ednildotorres@gmail.com

Abstract: Torrefaction has been investigated to improve the desirable properties of biomass as solid biofuel, usually used *in natura* as firewood in several countries. This paper has the main objective to present a broad characterization of the biomass *Prosopis juliflora* (*P. juliflora*), investigating its potential as a solid biofuel after its torrefaction process. The methodology was based on different procedures. The experimental runs were carried out at 230, 270, and 310 °C for 30 min, using a bench-scale torrefaction apparatus, with an inert atmosphere. In order to investigate the effect of temperature in constant time, torrefaction parameters were calculated, such as mass yield, energy yield, calorific value, base-to-acid ratio (B/A), and the alkaline index (AI). The physicochemical properties of the torrefied samples were determined and thermogravimetric analysis was used to determine the kinetic parameters at four different heating rates of 5, 10, 20, and 30 °C/min. Pyrolysis kinetics was investigated using the Flynn-Wall-Ozawa (FWO) and Kissinger-Akahira-Sunose (KAS) isoconversional methods. Highly thermally stable biofuels were obtained due to the great degradation of hemicellulose and cellulose during torrefaction at higher temperatures. The highest heating value (HHV) of the samples varied between 18.3 and 23.1 MJ/kg, and the energy yield between 81.1 and 96.2%. The results indicate that *P. juliflora* torrefied becomes a more attractive and competitive solid biofuel alternative in the generation of heat and energy in northeast Brazil.

Keywords: biomass; thermal treatment; pyrolysis; torrefaction; kinetics; biofuel; renewable energy



Citation: Carneiro-Junior, J.A.d.M.; de Oliveira, G.F.; Alves, C.T.; Andrade, H.M.C.; Beisl Vieira de Melo, S.A.; Torres, E.A. Valorization of *Prosopis juliflora* Woody Biomass in Northeast Brazilian through Dry Torrefaction. *Energies* **2021**, *14*, 3465. <https://doi.org/10.3390/en14123465>

Academic Editors: Marek Wróbel and Marcin Jewiarz

Received: 5 May 2021

Accepted: 6 June 2021

Published: 11 June 2021

Publisher's Note: MDPI stays neutral with regard to jurisdictional claims in published maps and institutional affiliations.



Copyright: © 2021 by the authors. Licensee MDPI, Basel, Switzerland. This article is an open access article distributed under the terms and conditions of the Creative Commons Attribution (CC BY) license (<https://creativecommons.org/licenses/by/4.0/>).

1. Introduction

About a third of the world's population, approximately 2.4 billion people, uses firewood for cooking, boiling water, and heating. Forests provide approximately 40% of global renewable energy in the form of fuel—roughly the combined use of solar, hydro, and wind energy [1]. Brazil is the largest producer of charcoal in the world, producing around 6.2 million tons in 2015, 12% of global production. More than 90% of the charcoal produced is from wood and it is the metallurgical industry that uses 80% of the total, unlike other countries where charcoal is used mainly in the food industry and in households [2]. There is great potential in Brazil for the use of woody biomass residues that could support the generation of energy with an installed capacity of about 6.5 GW/year, according to the Energy Research Company [3].

Biomass is an important renewable source that can contribute to the current challenge of reducing the use of fossil fuels, mitigating the emissions of greenhouse gases, nitrogen

oxides, and sulfur oxide. Biomass can be energetically converted into biofuels, in general, by the following technological routes: thermochemistry, biochemistry, and physicochemistry. The thermochemical route uses heat input to directly generate energy or to produce secondary fuels with higher energy density. The different thermochemical ways of obtaining energy from biomass include pyrolysis, gasification, co-combustion, and others. Among the various biomass conversion alternatives, thermochemical processes are widely applied in the production of bioenergy, frequently using torrefaction as a pre-treatment method for biomass [4,5].

In the past decade, various forms of biomass have been co-burned in coal-fired boilers and gas plants worldwide [6]. However, the economic viability of biomass co-burning with coal or natural gas is determined by the purchase and transport costs of each biomass [7]. Raw biomass usually has some undesirable characteristics, such as low energy density, high moisture, and hygroscopic nature, which generate high costs during handling and storage.

To overcome these difficulties, biomass torrefaction is a heat treatment technology suitable for energy purposes [8,9]. It consists of thermal pre-processing of biomass [4,5], which occurs at temperatures between 200 and 350 °C, in atmospheric conditions and the absence of oxygen. This improves some desirable characteristics of biomass, such as energy density, hydrophobicity, milling, storage, and logistical capacity [10]. As a consequence, the torrefied biomass retains a large part of its energy constituents, resulting in a higher percentage of carbon, greater calorific value and greater energy density [11].

Different torrefaction routes have been applied to improve and homogenize the physicochemical characteristics and the energetic properties of raw biomass for energy issues, such as wet processing [12,13], dry processing [8,14], and processing with ionic liquids [15,16]. Among them, dry torrefaction is the most used technology on a commercial scale and has attracted great interest as a pre-treatment to improve the properties of biomass before pyrolysis and gasification processes.

The genus *Prosopis* (*Leguminosae*, *Mimosoideae*) comprises about 44 species and its natural occurrence mainly covers North and South America, but there are also reports of the occurrence of some species in Africa and Asia. *Prosopis* was introduced in the northeastern semi-arid region of Brazil in 1942, as an economic alternative to traditional crops, as it grows on poor soils [17]. In the past few decades, different species of *Prosopis* have been widely introduced in various countries around the world to provide firewood and forage. The species include *P. glandulosa* and *P. velutina* in North America, and *P. chilensis*, *P. juliflora* and *P. alba* in South America. Three other species, *P. africana*, *P. cineraria*, and *P. tamarugo* are also important in their native areas [18]. The species *P. juliflora* currently occupies large areas in all states in the northeast of Brazil, with estimates above 500 thousand hectares in the semi-arid northeast [19]. This fact deserves a scientific study about the importance of its presence in the Brazilian semi-arid region.

Some works have been published on *Prosopis* wood torrefaction, each one using different approaches. Patel, et al. [20] investigated the improvement of biofuels derived from several raw materials, including *P. juliflora* after torrefaction at 300 °C, for 60 min, using statistical analysis to compare the parameters of proximate analyses. However, they did not report any effect of the torrefaction temperature on the physicochemical properties of this biomass. Eseltine, et al. [21] investigated the torrefaction of *Prosopis glandulosa* using thermogravimetric analysis (TG) in nitrogen and carbon dioxide atmospheres and observed greater degradation of hemicellulose and cellulose in carbon dioxide. Although they investigated several temperatures between 200 and 300 °C, and different particle sizes in the range of 2–4 mm, for a fixed residence time of 60 min, only the effect of inert and non-inert gases on biomass degradation was evaluated. Using surface response methods, Natarajan, et al. [22] reported that particle size and microwave power can affect the yield, calorific value, and energy recovery of the final product in the torrefaction of *P. juliflora* biomass at 150–250 °C. In addition to the few studies about *P. juliflora* torrefaction reported in the literature, they are also very limited to some specific conditions.

The study of torrefaction at different temperatures and the broad physicochemical and energetic characterization proposed here aims to present information that makes this biomass more attractive and commercially competitive. It also assists in the diversification of raw materials for the generation of biomass energy in more isolated regions and, indirectly, in eventual political-technical-administrative decision-making.

As far as we know, no one has thoroughly investigated the characterization of torrefied *P. juliflora*. In the present work, the effect of torrefying the biomass of *P. juliflora* wood is evaluated at 230, 270, and 310 °C, in nitrogen flow, for 30 min. The temperature effect can be seen in the weight loss characteristics and the variation of the biomass energy profile. The main physicochemical properties of the *P. juliflora* torrefied wood are determined and the pyrolysis kinetics is studied using TG curves and isoconversional methods. In addition, the potential to improve the properties of *P. juliflora* solid biofuel is evaluated.

2. Materials and Methods

2.1. Biomass and Preparation

The raw biomass of *Prosopis juliflora* was collected at the Irecê Campus of the Federal Institute of Bahia (IFBA), in the northeast region of Brazil (11°19'40" S, 41°52'01" W). Samples of the upper central branches, without shell, in cylindrical shapes (15–20 × 20 mm) were used. The biomass samples were dried in the sun for 72 h, ground in a Willye mill, sieved in a 40–50 mesh, and dried in an oven at 105 °C for 24 h.

2.2. Torrefaction Experiments

The torrefaction experimental runs were carried out in a fixed bed reactor (internal diameter of 4", length of 40 cm) with indirect heating and connected to a condensation system (Figure 1). The torrefaction reactor has thermal insulation of rock wool, a stainless-steel sample port and a collar type heating resistance with ceramic coating electrical resistance.

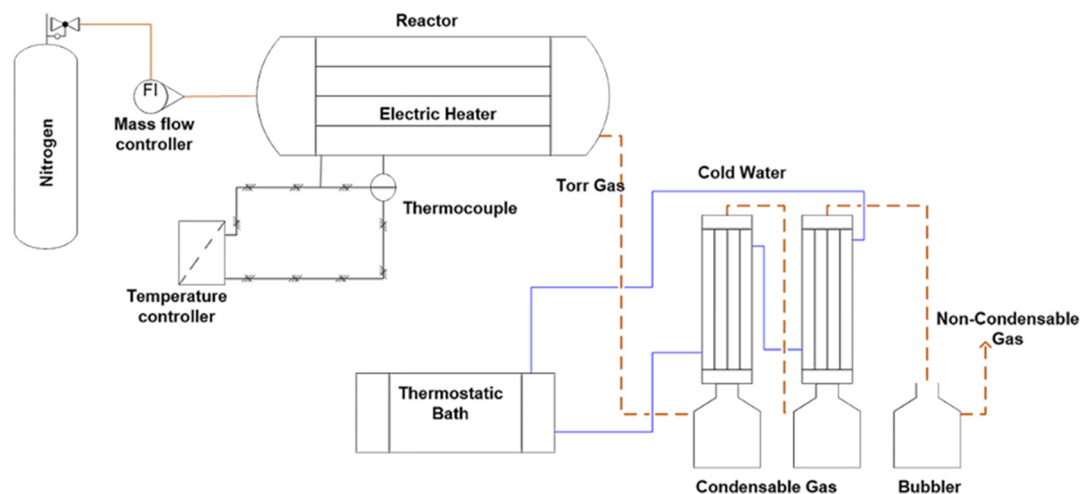


Figure 1. Bench-scale torrefaction apparatus.

Torrefaction experiments were carried out at 230, 270, and 310 °C ± 10 °C, 40 g/batch, the heating rate of 10 °C/min, 30-min isotherms, volumetric flow of 18 L/min of nitrogen, and 2 repetitions per treatment. The residence time does not affect the mass loss and the properties of the torrefied biomass [23]. At the end of each experiment, the samples were cooled inside the reactor to 50 °C and then placed in a desiccator to cool at room temperature. The torrefied samples were named PJ105, PJ230, PJ270, and PJ310, about the biomass of *Prosopis juliflora* (PJ) and drying temperature (105 °C) and torrefaction temperatures (230, 270, and 310 °C).

The mass loss, mass yield, energy yield, and energy density, after torrefaction at each temperature, were determined using Equations (1)–(4) [11,23].

$$\text{Weight loss} = \left(\frac{M_{\text{raw}} - M_{\text{torr}}}{M_{\text{raw}}} \right) \times 100, \quad (1)$$

$$\text{Mass yield} = \frac{M_{\text{torr}}}{M_{\text{raw}}} \times 100 \quad (2)$$

$$\text{Energy yield} = \text{Mass yield} \times \frac{\text{HHV}_{\text{torr}}}{\text{HHV}_{\text{raw}}} \quad (3)$$

$$\text{Energy density} = \frac{\text{Energy yield}}{\text{Mass yield}} \quad (4)$$

where M_{raw} is the mass of raw biomass (kg); M_{torr} is the mass of torrefied biomass (kg); HHV_{raw} is the higher heating value of raw biomass (MJ/kg); HHV_{torr} is the higher heating value of torrefied biomass (MJ/kg).

2.3. Biomass Characterization

All the proximate analyses were carried out by ASTM—American Society for Testing and Materials—technical standards. The moisture contents (MC), ash and volatile material (VM), and fixed carbon (FC) were respectively determined according to ASTM E871-82 (2019), ASTM E1755-01 (2020), ASTM E872-82 (2019), while fixed carbon (FC) was determined by subtracting the percentages of moisture, volatile matter, and ash from a sample. Then, MC, Ash, MV, and FC were calculated using Equations (5)–(8):

$$\text{MC}(\%) = \left(\frac{\text{initial mass of sample} - \text{final mass of sample}}{\text{final mass of sample}} \right) \times 100 \quad (5)$$

$$\text{Ash}(\%) = \left(\frac{\text{mass of residue}}{\text{initial mass of sample}} \right) \times 100 \quad (6)$$

$$\text{VM}(\%) = \left(\frac{\text{mass loss due to VM}}{\text{initial dry mass of sample}} \right) \times 100 \quad (7)$$

$$\text{FC} = 100 - \%(\text{MC} + \text{VM} + \text{Ash}), \quad (8)$$

ultimate analyses were performed according to ASTM E5291 (2016), using a Perkin Elmer 2400 Elemental Analyzer (series ii; Perkin Elmer, Boston, MA, USA). The oxygen content was calculated by subtracting the percentages of carbon (C), hydrogen (H), nitrogen (N), and ash, using Equation (9).

$$\text{O} = 100 - \%(\text{C} + \text{H} + \text{N} + \text{S} + \text{Ash}) \quad (9)$$

The apparent particle density (BD), defined as the mass of many particles of a material divided by the total volume they occupy, was determined according to ASTM E873-82 (2019). The total volume is the sum of the volume of the particles, the volume of the interparticle void, and the internal pore volume. The apparent particle density (g/cm) was calculated by Equation (10).

$$\text{BD} = \frac{\text{Weight Sample}}{\text{Volume Beaker}} \quad (10)$$

The main oxides in the biomass ash were determined in X-ray dispersive energy spectrometry, using analytical curves for quantitative analyses. Then, the base-to-acid ratio (B/A) and the alkaline index (AI) were calculated using Equations (11) and (12) [24,25]:

$$\frac{\text{B}}{\text{A}} = \frac{\text{Fe}_2\text{O}_3 + \text{CaO} + \text{MgO} + \text{K}_2\text{O} + \text{Na}_2\text{O} + \text{P}_2\text{O}_5}{\text{SiO}_3 + \text{TiO}_2 + \text{Al}_2\text{O}_3} \quad (11)$$

$$AI = \frac{(Na_2O + K_2O)_{fuel, dry\ basis}}{HHV_{dry\ basis}} \left(\frac{kg}{GJ} \right) \quad (12)$$

The highest heating value (HHV) was measured in an IKA C2000 basic calorimeter pump, using 1.0 g of dry biomass and an oxygen atmosphere, by ASTM D2015/2000.

2.4. Thermogravimetric Analyses

The thermal decomposition of the samples was investigated in thermogravimetric analysis equipment, TG-DTA Shimadzu DTG-60H (Shimadzu Corp., Kyoto, Japan), in the range of 30–1000 °C, with an accuracy of ± 2 °C and microbalance sensitivity of 0.001 mg. The experiments were carried out under an inert atmosphere, nitrogen flow of 50–100 mL/min, variable heating rate, using 10 mg of sample mass placed in a platinum crucible. The samples were previously dried, milled, and sieved through a 0.2 mm sieve. The temperature was initially maintained for 5 min to remove free moisture and provide a dry basis for thermal analysis. Then, the experiment was carried out with heating rates of 5, 10, 20, and 30 °C/min.

2.5. Kinetic Analyses

The kinetic parameters of thermal decomposition of the biomass are based on the determination of the triad pre-exponential factor, activation energy, and reaction order. In general, the thermal decomposition of the biomass can be described by Equation (13),

$$\frac{d(\alpha)}{dt} = kf(\alpha) \quad (13)$$

where k is the reaction rate constant, $f(\alpha)$ is the usual kinetic model for solids conversion, and α represents the mass loss fraction obtained through the TG/DTG curve, expressed by Equation (14):

$$\alpha = \frac{m_0 - m_t}{m_0 - m_f} \quad (14)$$

where m_0 is the sample initial mass, m_f is the final mass, and m_t is the sample mass as a function of time (t). k is a function of temperature following Arrhenius Equation (15):

$$k = A \exp(-E_a/RT) \quad (15)$$

where A is the frequency or pre-exponential factor (s^{-1}), E_a is the activation energy of the decomposition reaction (kJ/kmol), R is the universal gas constant (kJ/(kmol \times K)), and T is the temperature (K).

For non-isothermal kinetics, the usual case of linear heating corresponds to a constant heating rate. Combining Equations (13) and (15), the result in Equation (16):

$$\frac{d\alpha}{dt} = \frac{A}{\beta} \exp(-E_a/RT) f(\alpha) \quad (16)$$

The Flynn–Wall–Ozawa (FWO) and Kissinger–Akahira–Sunose (KAS) isoconversional methods were developed on the assumption of a reaction mechanism or by empirical adjustment [26]. Isoconversional methods have the main advantage over model-fitting and single-heating-rate methods, the absence of any reaction models for the calculation of activation energy. The analysis of the approach is essentially free of reaction models. Thus, for complex materials such as biomass, where the reaction occurs at different stages and the decomposition mechanism is susceptible to variations, isoconversional methods are ideally suited [27], accurate, and save time compared to the model-fitting method [28].

The FWO method uses the integral form of the non-isothermal rate equation (16), based on Doyle's approximation, as shown in Equation (17):

$$\log(\beta) = \log\left(\frac{AEa_i}{Rg(\alpha)}\right) - 2.315 - 0.4567\frac{E_a}{RT_{\alpha_i}} \quad (17)$$

Subscripts i and α denote a given value of heating rate and fractional conversion, respectively. The activation energy (E_a) can be determined from the slope $-0.4567\frac{E_a}{R}$ and the pre-exponential factor value (A) can be calculated from the intercept of a $\log(\beta)$ against $\frac{1}{T_{\alpha_i}}$ plot. The $g(\alpha)$ is constant at a given conversion value. The KAS model is more widely used for kinetic studies of biomass pyrolysis [29] and the solution of the mathematical approximation for the exponential term is given by Equation (18):

$$\ln\left(\frac{\beta_i}{T_{\alpha_i}^2}\right) = \ln\left(\frac{A_{\alpha}Ea_{\alpha}}{Rg(\alpha)}\right) - \frac{E_a}{RT} \quad (18)$$

The kinetic parameters are determined graphically by plotting $\ln\left(\frac{\beta_i}{T_{\alpha_i}^2}\right)$ as a function of $1/T$ for the fixed conversion value α , where the slope is equal to $-E_a/R$. In addition, the apparent activation energy ($E_{a\alpha}$) can be determined by replacing the values of the variables ($g(\alpha)$ and A , intercept) and the R-value as 8.3145 kJ/(kmol \times K). The activation energy is obtained for the entire conversion interval (0.1–0.8).

Although the KAS method is considered more accurate than the FWO equation [30], the kinetic parameters obtained from different isoconversional methods show little variation [26]. Therefore, both methods were used to describe the torrefaction kinetics of *P. juliflora* comparatively at the heating rates of 5, 10, 20, and 30 °C/min. Matlab® software (2017b; Natick, MathWorks Inc., MA, USA) was used to estimate the pre-exponential factor and the activation energy and fit the kinetic model to the measured experimental data. The results provide relevant information for understanding the torrefaction of *P. juliflora* biomass at different temperatures.

3. Results

3.1. Torrefaction Process

Table 1 shows the average gravimetric yield of the torrefied products (PJ230, PJ270, and PJ310). These results are in agreement with the literature [20,31], which reports that the mass yield of a solid product strongly depends on the torrefaction temperature, the reaction time, and the type of biomass.

Table 1. Yields of torrefaction tests.

Process Yield	PJ230	PJ270	PJ310
Mass Yields (%)	88.2 \pm 0.6	77.1 \pm 1.2	64.5 \pm 1.2
Liquid Yields (%)	10.3 \pm 1.1	15.5 \pm 1.5	23.4 \pm 1.9
Bulk Density * (g/cm)	0.807 \pm 0.012	0.722 \pm 0.025	0.659 \pm 0.029

* Apparent particle density.

The volatiles that leave the reactor pass through a condenser system where one part is condensed and the other part is bubbled into the water before exhaustion. The mass yields of solids obtained at 230, 270, and 310 °C correspond to 88.2%, 77.1%, and 64.5% of the raw biomass, respectively. The reduction in solids yield with increasing temperature was also observed by Acharya and Dutta [10], and the torrefaction modifies the biomass composition. It is generally accepted that hemicellulose degradation occurs at temperatures above 200 °C, lignin slowly decomposes at approximately 160–900 °C [32], while cellulose decomposition occurs between 200 and 400 °C. The decomposition of hemicellulose was identified as the dominant reaction during the biomass torrefaction [33], most of the

biomass mass loss can be attributed to the decomposition of hemicellulose into volatile compounds. Cardona, Gallego, Valencia, Martínez, and Rios [14] obtained 77 ± 5 , 72 ± 5 and $55 \pm 4\%$ by weight after 40 min torrefaction of different eucalyptus residues at 250, 275, and 300 °C, respectively. Natarajan, Suriapparao, and Vinu [22] obtained 15–30% by weight of volatile yields, and 72.5%, 80% and 69.4% by weight of solids yields, after torrefaction of 2–4 mm particles of *P. juliflora*, using a microwave oven with values of MW power of 300, 450, and 600 W, respectively.

The apparent particle density of the samples at PJ105, PJ230, PJ270, and PJ310 correspond to 0.839, 0.807, 0.722, and 0.659 g/cm, respectively. The reduction of the porosity and humidity with the increase of the torrefaction temperature results in the increase of the apparent densities. According to Saeed, et al. [34], with the decomposition of hemicellulose and the increase in the lignin content during the torrefaction process, there is an improvement in the biomass compaction capacity and, consequently, an increase in apparent densities.

The color changes of torrefied *P. juliflora* wood at different temperatures can be seen in Figure 2 and are related to losses of free surface moisture, internal moisture, and volatiles in the different steps of torrefaction [35].



Figure 2. Biomass of *P. juliflora* before and after torrefaction.

In addition to the conditions of the torrefaction process, several factors affect the final color of the torrefied biomass. The color changes of thermally treated biomass are mainly due to hydrolysis and oxidation reactions, considering the transport phenomena involved. Furthermore, color changes also depend on the type and density of crude biomass [36], along with the concentration of low molecular weight sugars, sugar alcohols, and nitrogenous compounds in wood [35].

3.2. Physicochemical Characterization

Torrefied biomass generally has more uniform physicochemical properties that are attractive for process optimization, control, and standardization of the biomass energy production chain [9]. The torrefaction temperature has a strong influence on the physical and chemical characteristics of the torrefied *P. juliflora*. During the biomass torrefaction process, partial removal of the hydroxyl groups (OH) is achieved by dehydration and prevents the formation of hydrogen bonds, resulting in an increase in the hydrophobia of the biomass particles [37]. The moisture content (air-dry basis) obtained for samples PJ105, PJ230, PJ270, and PJ310 were 6.1%, 0.3%, 0.1%, and 0.1%, respectively. The reduction of the moisture content and volatile material of the biomass has many positive results, such as the reduction in the cost of transportation, stable storage for a longer period, with a low risk of biological deterioration [7]. As shown in Figure 3, the volatile material decreases with increasing the torrefaction temperature, producing more stable biofuels.

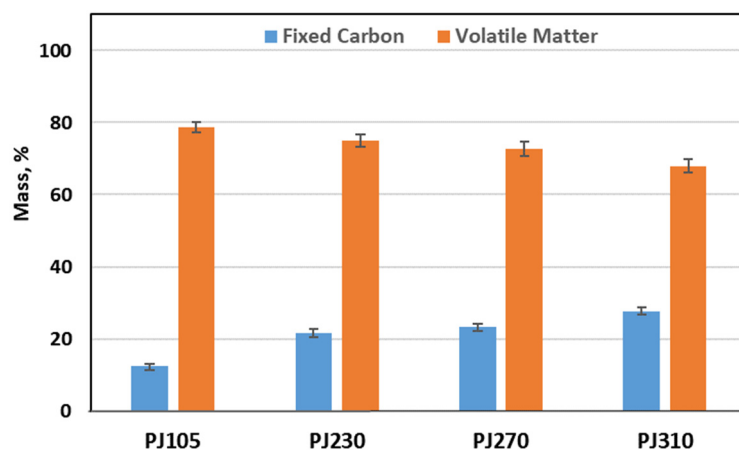


Figure 3. Profiles of the volatile matter and fixed carbon of *P. juliflora* samples.

The increase in the torrefaction temperature to 310 °C led to an increase in fixed carbon (FC) from 12.35 to 27.66%. The measured torrefaction experimental data follow those reported in the literature [22,38,39]. Low VMs and ignition and combustion temperatures are among the main advantages of biomass for thermochemical conversion and are important criteria for the highly reactive nature of this fuel [40].

Figure 4 shows the profiles with the higher heating value (HHV) and ash from the samples torrefied at different temperatures. The HHV for PJ105, PJ230, PJ270, and PJ310 were 18.33, 20.01, 21.14, and 23.05 MJ/kg, respectively.

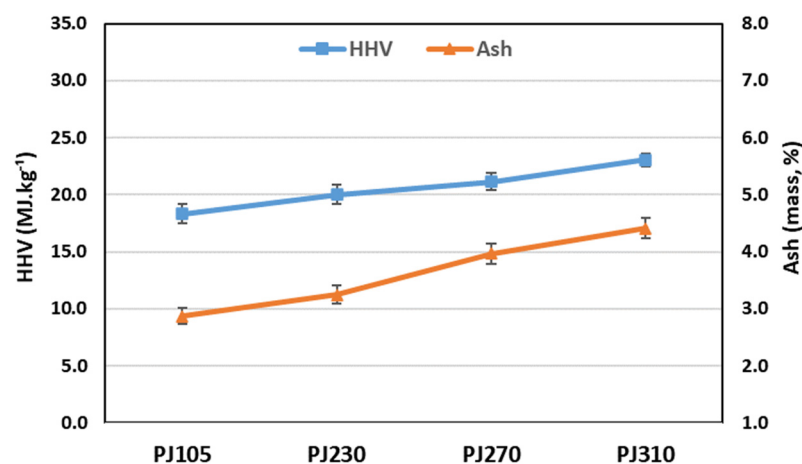


Figure 4. Profiles of the HHV and ash content of the *P. juliflora* samples.

The HHV increased as a result of the increase in carbon content with an increase in the torrefaction temperature. It was observed that even at higher torrefaction temperatures (i.e., 310 °C), the coal still has a much higher HHV, in the range of 14–21 MJ/kg, mainly due to the significantly higher oxygen content of the biomass. In the torrefaction process, oxygen, with a negative contribution to the calorific value, is removed from the biomass reacting with hydrogen to form mainly H₂O and, with volatile carbon, to form mainly CO₂ [12]. This results in an energy-dense solid fuel with greater calorific power compared to crude biomass.

Chandrasekaran, et al. [41], Naseeruddin, et al. [42], and Suriapparao, Pradeep and Vinu [39] reported *P. juliflora* higher heating values (HHV) of 17.96, 16.90, and 17.02 MJ/kg, respectively, while Pereira and Lima [43] reported HHV of 19.35–21.47 MJ/kg in a study of six species of *Prosopis*. The behavior of increasing HHV with increasing the torrefaction temperature is already documented in the literature. Thus, the results obtained in the present study were expected, with pretreatment in the temperature range between 270 and

310 °C suggested as optimal conditions for the torrefaction of *P. juliflora* when considering the improvement of the energy source as a solid fuel. The ash content of biomass is generally small, but it can play a significant role in the use of biomass, especially if it contains alkali metals like potassium or halides like chlorine [23]. The ash mass fraction usually remains unchanged during torrefaction, while organic matter degrades during torrefaction and leads to a higher ash concentration [44]. For samples PJ230, PJ270, and PJ310, ash content values of 3.25, 3.97, and 4.41% were obtained, respectively. The composition of raw and torrefied *P. juliflora* ash is discussed in the next section. The results of the physicochemical characterization of raw and torrefied biomass samples and the Van Krevelen diagram, are detailed in Table S1 and Figure S1, respectively, of the Supplementary Materials.

An important parameter of torrefaction is the energy yield, which indicates how much energy remains in the torrefied biomass. In general, for improved biomass with high HHV, a lower mass yield is necessary to generate a solid fuel with better quality [45]. The results of energy and mass yield are shown in Figure 5. Similar to the values of mass yield (88.2%, 76% and 64.5%), the energy yield decreases (from 96.2 to 81.1%) with increasing torrefaction temperature.

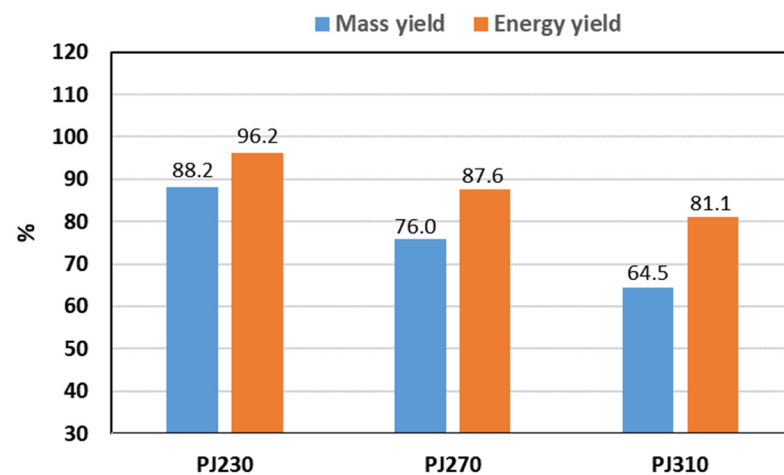


Figure 5. Mass and energy yields for the torrefaction the 203, 270, and 310 °C.

For all torrefied products, the energy yield was higher than the mass yield—an effect that was more evident for the treatment with a temperature of 310 °C, with a 16.6% greater difference between energy yield and mass yield. These results suggest a linear relationship between the outputs. Bach, et al. [46] obtained a mass yield of 74% in dry torrefaction at 275 °C for 60 min or through wet torrefaction at 222 °C for 5 min or at 210 °C for 30 min, for Norway spruce biomass. In another study of conventional torrefaction, for coffee grounds and microalgae residue, Ho, et al. [47] obtained mass yields in the range of 55.43–98.20% and 56.42–92.41%, respectively. It should be noted that the lower mass yield may be desirable if the energy yield is within an acceptable range. Comparatively, under equivalent temperatures, the biomass of *P. juliflora* torrefied shows promising mass and energy yields as a solid fuel.

The results of ultimate analyses of the raw and torrefied *P. juliflora* samples are presented in Table 2. The ultimate analysis of the torrefied samples reveals changes that occur in the chemical composition of the biomass when exposed to the torrefaction conditions, whose carbon content increased, while decreases were observed in the content of hydrogen and oxygen. The nitrogen content remained almost constant, considering the statistically standard deviation.

Table 2. Ultimate analyses of *P. juliflora* samples.

Samples	C	H	N	O	O/C	H/C
PJ105	46.30 ± 0.10	7.49 ± 0.05	0.25 ± 0.02	42.99 ± 0.50	0.70	1.94
PJ230	53.84 ± 0.15	6.45 ± 0.07	0.24 ± 0.02	36.21 ± 0.45	0.50	1.44
PJ270	61.24 ± 0.08	5.64 ± 0.10	0.10 ± 0.04	29.04 ± 0.90	0.36	1.11
PJ310	63.65 ± 0.05	5.23 ± 0.50	0.08 ± 0.04	26.62 ± 0.85	0.31	0.99

The results presented for HHV illustrate the impact that changes in elementary components have on energy content (Figure 5). During the reactions that occur in the torrefaction, the released compounds contain higher proportions of oxygen and hydrogen than the carbon, reducing the relative concentration of these elements in the solid fuel.

Wang, et al. [48] proposed that dehydration and dissociation were the main reactions of hemicellulose at lower temperatures, while depolymerization and fragmentation of residual monosaccharides occur at higher torrefaction temperatures. In addition, Neupane, et al. [49] observed that torrefaction causes the cleavage of aryl-ether bonds and de-methoxylation of lignin. Thus, these reactions favor an increase in the carbon content and, consequently, an increase in the higher calorific value.

The hydrogen-carbon (H/C) and oxygen-carbon (O/C) ratios are commonly used as indicators of energy densification during the torrefaction process [50]. On the other hand, the torrefied biomass becomes hydrophobic and, therefore, cannot retain or absorb free moisture, inhibiting biological decomposition [51]. The H/C and O/C ratios decreased with increasing temperature and with increasing carbon content.

Thus, the sample torrefied at 310 °C (PJ310) has an atomic composition close to that of lignite and coal [52], while that of the sample torrefied at an intermediate temperature (PJ270) is close to peat charcoal [6]. The H/C ratios between 0.9 and 1.9, obtained for PJ310 and PJ105, respectively, are consistent with the H/C ratios (1.1–1.4), presented by Suriapparao, Pradeep, and Vinu [39], for *P. juliflora* torrefied in a microwave oven under different experimental conditions.

Chandrasekaran, Ramachandran, and Subbiah [41] reported H/C ratios between 1.6 and 2.0, for dry and wet *Prosopis*, respectively. On the other hand, torrefied biomass becomes mechanically more fragile when H/C and O/C ratios are reduced [45]. Thus, it becomes a more suitable fuel for spraying in combustion systems [53] and requires less energy for grinding compared to crude biomass, as reported by Ohliger, et al. [54].

3.3. Inorganic Composition

Table 3 shows the inorganic composition of raw and torrefied *P. juliflora* ash. The predominance of Ca, K, and Fe in *P. juliflora* ash is characteristic of woody biomass [41,55].

Table 3. Inorganic composition of the ash of samples (% dry basis).

Biomass	SiO ₂	K ₂ O	CaO	MgO	Na ₂ O	P ₂ O ₅	Al ₂ O ₃	Fe ₂ O ₃	SO ₃	Others	B/A	AI
PJ105	0.034	0.512	1.654	0.142	0.009	0.054	0.022	0.398	0.026	0.028	0.274	0.507
PJ230	0.043	0.547	2.128	0.124	0.008	0.042	0.025	0.318	0.012	0.011	0.382	0.391
PJ270	0.052	0.629	2.725	0.136	0.010	0.047	0.025	0.313	0.014	0.030	0.348	0.382
PJ310	0.056	0.723	3.066	0.135	0.011	0.048	0.026	0.305	0.014	0.036	0.355	0.368

Note: AI = alkali index (kg/GJ); B/A = base-acid ratio.

The formation of slag and scale in thermal systems operated with biomass is commonly related to biomass ash. The B/A ratio is an important characteristic of solid biofuels, as a high percentage of basic oxides reduces the melting temperature of the ash, while that of acid oxides increases it [24]. Thus, alkalis in biomass ash contribute to the formation of slag and scale in combustion systems. Karampinis et al. (2012), Vamvuka and Kakaras (2011) [25,56] reported a tendency for scale formation in combustion systems when a B/A < 0.5, the tendency to deposit is low; medium, for 0.5 < B/A < 1 and high, for ratio B/A > 1. On the other hand, the alkali index (AI) allows a more accurate evaluation of the tendency of slag and scale formation, such that a high trend is predicted when

$0.17 < AI < 0.34$ kg/GJ [57]. Despite this, this trend strongly depends on the characteristics of each biomass and the combustion conditions. B/A and AI of the samples were calculated using the data presented in Table 3 and Equations (11) and (12), respectively.

As shown in Table 3, the B/A ratio increased from 0.274 to 0.355, which can be explained by the fact that the organic matter was decomposed, thus leaving the inorganic material. Alkaline Index (AI) decreased with increasing torrefaction temperature, from 0.507 to 0.368, decreasing the tendency for scale and slag deposition. Sample PJ105 showed $B/A < 0.5$, as reported for Greek lignite, a fossil fuel, and for poplar, woody biomass [25]. In general, samples PJ230, PJ270, and PJ310 showed a low slag deposition trend, showing B/A ratios lower than those reported by Vamvuka and Kakaras [56] for olive kernels (1.54) and waste wood (1.06) biomasses. On the other hand, *P. juliflora* samples showed AI in the range of 0.17–0.340 kg/GJ, indicating a high tendency to deposit slag.

3.4. Thermogravimetric Analyses and Pyrolysis Kinetic

It is generally accepted that the pyrolysis of biomass consists of three main steps: (i) initial evaporation of free moisture, (ii) primary decomposition followed by (iii) secondary reactions (oil cracking and depolymerization) [26,58,59]. Chandrasekaran, Ramachandran, and Subbiah [38] conducted TG and DTG experiments for *P. juliflora* crude performed at a maximum temperature of 600 °C, at six different heating rates of 2, 5, 10, 15, 20, and 25 °C/min in an argon atmosphere. Mythili, et al. [60], presented the thermogravimetric curve of Prosopis wood, with no variation in the heating rate, at a maximum temperature of 800 °C. Although these studies supported the analysis of crude biomass, it is important to note the lack of information on the behavior of pyrolysis of *P. juliflora* torrefied at different temperatures.

The pyrolysis of samples PJ105, PJ230, PJ270, and PJ310 was investigated using TG curves obtained in a nitrogen flow and heating rates of 5, 10, 20, and 30 °C/min, as shown in Figure 6. The range of mass loss attributed to residual moisture and adsorbed gases was 100–120 °C, being more related to PJ105. In general, for the samples, the thermal devolatilization stage started around 180–200 °C, followed by a great loss of mass around 200–640 °C, and by a flat flow zone that depends on the torrefaction temperature used (230, 270, or 310 °C). The thermal devolatilization events of hemicellulose, cellulose and lignin are often observed between 220–315 °C, 315–400 °C, and 180–850 °C [23,27], respectively, but some variations can occur between the different types of biomass.

It is observed that the samples show quantitative variations in the devolatilization stage due to differences in the chemical composition caused by the temperature of the thermal pre-treatment of the torrefaction. In general, thermograms with heating rates of 5 and 10 °C/min are characterized by two devolatilization zones indicated in the DTG curves. The well-defined main peak is attributed to the primary hemicellulose zone and incomplete cellulose decomposition, followed by the sub-peak that assigns the secondary zone to lignin and the rest of the biomass degradation, as observed in the literature [61].

Di Blasi [62] reported that lower heating rates affect the dynamics of the components and can generate several zones that appear on the mass loss curves. In addition, the gradual heating of the biomass over a sufficiently long time increases the efficiency of heat transfer to the internal portions of the biomass particles.

The mass loss of crude biomass, PJ105, was greater than that observed for samples PJ230, PJ270, and PJ310, due to the progressive removal of hemicelluloses during the torrefaction process. The thermogram profile reveals that less mass loss is obtained when the temperature of the pre-treatment of the biomass is higher (230, 270, or 310 °C). The amount of solid product, in a TG run at 10 °C/min, increased significantly from 22.4% to 25.4%, 43.4% and 59.3% with the torrefaction temperature of 230, 270, and 310 °C, respectively, as shown in Figure 6 and Table 4. As a result, more thermally stable biofuels are obtained due to the great degradation of hemicelluloses and cellulose during torrefaction at high temperatures.

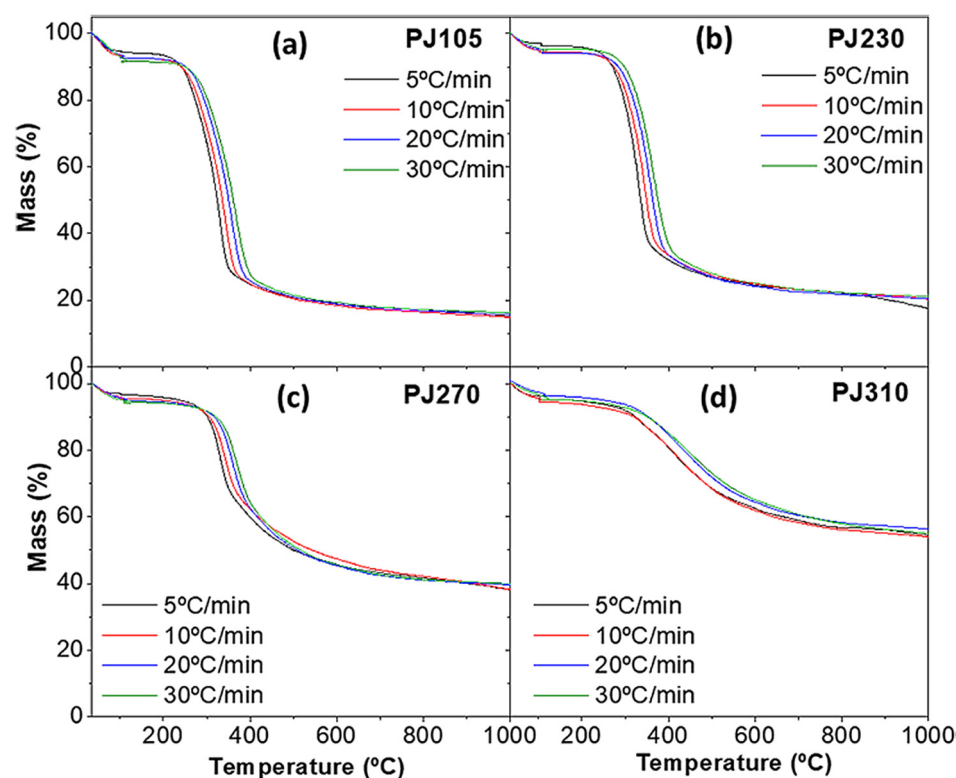


Figure 6. TG profiles of *P. juliflora* samples at different heating rates of 5, 10, 20, and 30 °C/min for (a) raw biomass—PJ105; (b) PJ230; (c) PJ270; (d) PJ310.

Table 4. Devolatilization percentages of *P. juliflora* samples.

Heating Rate	Devolatilization (%)			
	PJ105	PJ230	PJ270	PJ310
5	78.5	77.4	57.4	39.8
10	77.6	74.6	56.6	40.7
20	77.4	74.3	55.6	40.4
30	75.1	74.1	54.8	40.3

As a result, there is an improvement in cracking biomass, leading to increased degradation and loss of mass in the form of volatile components. On the other hand, as the heating rate increases, the peaks generated in the DTG curve increase progressively, as can be seen in Figure 7.

The loss of mass due to devolatilization is shown in the derivative profile by the shoulder- and peak-shaped curves, corresponding to the decomposition of hemicellulose and cellulose, and then another small deformation at high temperature related to lignin is reported in the literature [61,63]. The gradual disappearance of the shoulders, respectively in samples PJ230, PJ270, and PJ310, occurring in the range of 220–320 °C, is an indication of possible degradation of holocellulose and other components as the pre-treatment temperature increases [33,63]. The smoothing of the curves was observed by Cao, Yuan, Jiang, Li, Xiao, Huang, Chen, Zeng, and Li [5].

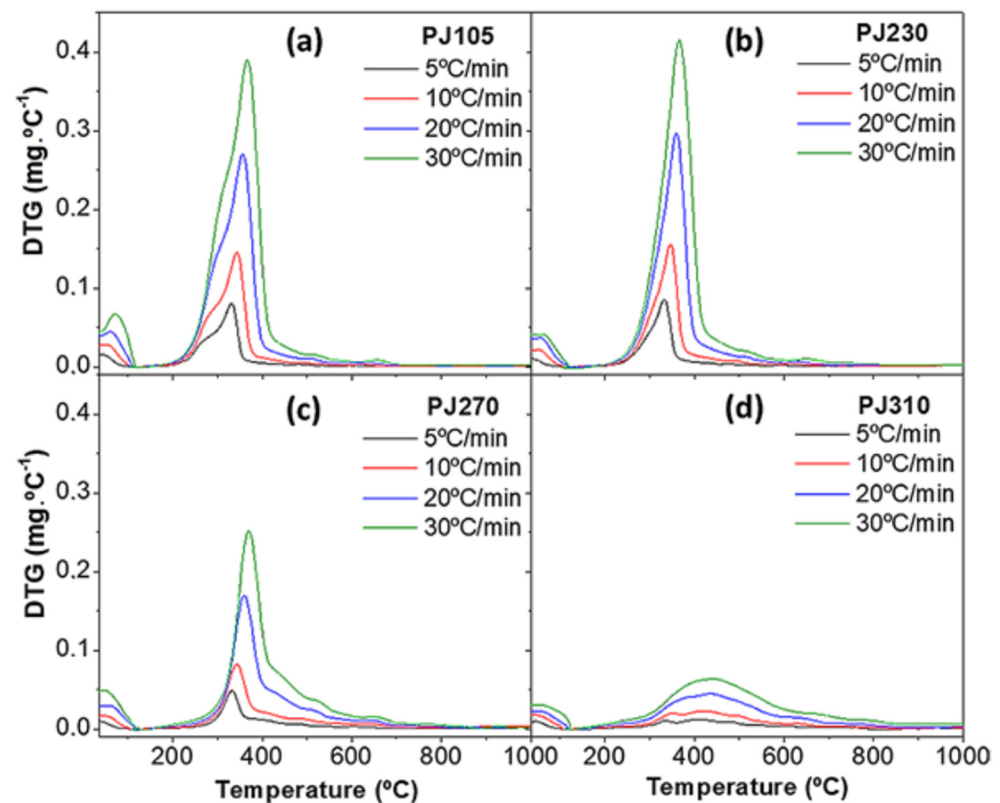


Figure 7. DTG profiles of *P. juliflora* samples at different heating rates of 5, 10, 20, and 30 °C/min for (a) raw biomass—PJ105; (b) PJ230; (c) PJ270; (d) PJ310.

The gradual heating of biomass for an adequate time changes the efficiency of heat transfer to the internal portions of the biomass particles, resulting in different biomass degradation and mass loss as volatile components [26,59]. To be useful as a biofuel, biomass must be depolymerized and deoxygenated [64]. References [65–68] are related to the Supplementary Materials.

The data obtained in the TG experiments (Figure 6) were used to fit the kinetic model. The FWO and KAS methods were used to calculate the kinetic parameters of pyrolysis of *P. juliflora* samples. The activation energies for each conversion can be obtained from the slope of $\log \beta$ versus $1/T$ graphs. The FWO and KAS methods were applied to the data sets in the conversion range of 0.1–0.8, but the correlation values are low at conversion ranges below 0.2 and above 0.7, leading to inaccurate kinetic data. Each regression line, derived from Equations (17) and (18), represents the activation energy, the average of which is shown in Table 5.

Table 5. Kinetic parameters obtained from FWO and KAS methods for samples.

Sample	FWO Model			KAS Model		
	E_a (kJ/kmol)	A (s ⁻¹)	R^2	E_a (kJ/kmol)	A (s ⁻¹)	R^2
PJ105	144.8	2.70×10^{15}	0.9958	142.4	4.19×10^6	0.9952
PJ230	149.7	4.16×10^{15}	0.9982	147.5	6.16×10^6	0.9979
PJ270	180.2	1.17×10^{28}	0.9653	179.2	1.40×10^{19}	0.9616
PJ310	261.0	3.82×10^{25}	0.9611	263.1	3.39×10^{16}	0.9677

The kinetic parameters obtained by the two isoconversional models show little variation, which can be attributed to different approximations of the temperature integral used as the solution, calculated by Equations (17) and (18). The obtained results, using both

models, do not significantly differ in the conversion range of 0.2–0.7. Table 5 shows the values of activation energy (E_a), pre-exponential factor (A), and correlation coefficient (R^2).

The biomass PJ105, PJ230, PJ270, and PJ310 showed average values of E_a of 144.8, 149.7, 180.2, and 261.0 kJ/kmol for FWO and, 142.4, 147.5, 179.2, and 263.1 kJ/mol for KAS. For dry biomass (PJ105), the values of E_a at the beginning of pyrolysis were lower than those of torrefied biomass. The activation energy increased with torrefaction temperatures due to changes in the internal structures of biomass, such as the degradation of holocellulose and other components.

As observed in this work (Figure 7) and reported by Doddapaneni, Konttinen, Hukka, and Moilanen [28], Chen and Kuo [33], the increase in activation energy can be attributed to the depletion of hemicellulose during the torrefaction process. As the reactive hemicellulose is completely degraded, the pyrolysis of the torrefied biomass at high temperatures (PJ310) requires more energy to initiate the pyrolysis reactions.

The FWO and KAS methods correlated satisfactorily with the pyrolysis kinetics of *P. juliflora*, with the correlation coefficients (R^2) obtained higher than 0.96, and the activation energy of the samples increased with the torrefaction temperature. The KAS graphs showed similar behavior to those plotted for FWO, maintaining the same variation in the results obtained. The activation energy of raw *P. juliflora* pyrolysis was determined using the models by Kissinger, KAS, FWO, and Friedman, reported by Chandrasekaran, Ramachandran, and Subbiah [38], and the values reached 164.6, 204.0, 203.2, and 219.3 kJ/kmol, respectively. Doddapaneni, Konttinen, Hukka, and Moilanen [28] observed for the torrefied biomass of *Eucalyptus urophylla* at 250, 275, and 300 °C, the respective values of 183, 184, and 196 kJ/kmol for FWO; 182, 183, and 195 kJ/kmol for KAS.

The results also indicate that the torrefaction temperature has a significant effect on the pyrolysis kinetics of torrefied *P. juliflora*. Under more severe torrefaction conditions, the biomass structure is significantly affected and, in turn, the decomposition kinetics of the biomass components. In addition, the analysis of kinetic parameters is also influenced by several factors, such as the temperature range of pyrolysis, mathematical analysis method, pyrolysis techniques, particle size, and chemical composition of the biomass sample [5].

4. Conclusions

The torrefaction of *P. juliflora* was investigated at 230, 270, and 310 °C, in a fixed bed reactor, using cylindrical samples of 15–20 × 20 mm. After torrefaction at 270 and 310 °C, the samples showed higher levels of fixed carbon, energy density and HHV, in addition to low H/C and O/C ratios. This indicates that these samples are hydrophobic and, therefore, unable to retain or absorb free moisture, inhibiting biological decomposition. On the other hand, the ash composition led to B/A ratios and AI indexes comparable to those reported for other woody biomasses and indicate a moderate tendency for scale and slag formation. The kinetic parameters of pyrolysis, determined by the isoconversional FWO and KAS methods, were comparable to those reported in the literature and varied between 144 and 244 kJ/kmol. Figures S2 and S3 of the Supplementary Materials present the activation energy estimation data using the FWO and KAS isoconversional methods. The characteristics observed for torrefied *P. juliflora* woody biomass potentiate it as a solid biofuel, being able to be used as an input in thermo-conversion processes, unconventional raw material, or precursor in the production of liquid and gaseous biofuels. It is interesting to highlight that conducting future research on the economic viability and densification of torrefied *P. juliflora* biomass can undoubtedly benefit local producers, cooperatives, and enterprises, as this research can be incorporated into a regional development plan.

Supplementary Materials: The following are available online at <https://www.mdpi.com/article/10.3390/en14123465/s1>, Table S1: physicochemical characterization of *P. juliflora* samples, Figure S1: Van Krevelen diagram of the *P. juliflora* samples, Figure S2: Estimation of activation energy using the FWO isoconversional method, Figure S3: Estimation of activation energy using the KAS isoconversional method.

Author Contributions: Conceptualization, J.A.d.M.C.-J., E.A.T. and H.M.C.A.; methodology, J.A.d.M.C.-J., G.F.d.O. and H.M.C.A.; validation, J.A.d.M.C.-J., C.T.A. and H.M.C.A.; formal analysis, J.A.d.M.C.-J.; investigation, J.A.d.M.C.-J. and G.F.d.O.; resources, E.A.T. and J.A.d.M.C.-J.; data curation, H.M.C.A.; writing—original draft preparation, J.A.d.M.C.-J., H.M.C.A. and G.F.d.O.; writing—review and editing, S.A.B.V.d.M., H.M.C.A. and E.A.T.; supervision, C.T.A. and S.A.B.V.d.M.; funding acquisition, E.A.T. and J.A.d.M.C.-J. All authors have read and agreed to the published version of the manuscript.

Funding: This research was funded by Energy and Gas Laboratory of the Federal University of Bahia—Brazil, and was carried out with the support of the Coordination for the Improvement of Higher Education Personnel—Brazil (CAPES)—Financing Code 001.

Institutional Review Board Statement: Not applicable.

Informed Consent Statement: Not applicable.

Data Availability Statement: Not applicable.

Acknowledgments: This work was carried out with the support of the Coordination for the Improvement of Higher Education Personnel—Brazil (CAPES)—Financing Code 001.

Conflicts of Interest: The authors declare no conflict of interest. The funders had no role in the design of the study; in the collection, analyses, or interpretation of data; in the writing of the manuscript, or in the decision to publish the results.

References

- Messerli, P.; Murniningtyas, E.; Eloundou-Enyegue, P.; Foli, E.G.; Furman, E.; Glassman, A.; Hernández Licona, G.; Kim, E.M.; Lutz, W.; Moatti, J.-P. *Global Sustainable Development Report 2019: The Future Is Now—Science for Achieving Sustainable Development*; United Nations: New York, NY, USA, 2019.
- FAO. *The State of the World's Forests—Forest Pathways to Sustainable Development*; Food and Agriculture Organization of the United Nations: Rome, Italy, 2018.
- EPE. *Potential Energético de Resíduos Florestais do Manejo Sustentável e de Resíduos da Industrialização da Madeira*; Ministério de Minas e Energia: Brasília, Brazil, 2018.
- Álvarez, A.; Nogueiro, D.; Pizarro, C.; Matos, M.; Bueno, J.L. Non-oxidative torrefaction of biomass to enhance its fuel properties. *Energy* **2018**, *158*, 1–8. [[CrossRef](#)]
- Cao, L.; Yuan, X.; Jiang, L.; Li, C.; Xiao, Z.; Huang, Z.; Chen, X.; Zeng, G.; Li, H. Thermogravimetric characteristics and kinetics analysis of oil cake and torrefied biomass blends. *Fuel* **2016**, *175*, 129–136. [[CrossRef](#)]
- Agbor, E.; Zhang, X.; Kumar, A. A review of biomass co-firing in North America. *Renew. Sustain. Energy Rev.* **2014**, *40*, 930–943. [[CrossRef](#)]
- Kumar, L.; Koukoulas, A.A.; Mani, S.; Satyavolu, J. Integrating torrefaction in the wood pellet industry: A Critical Review. *Energy Fuels* **2017**, *31*, 37–54. [[CrossRef](#)]
- Arteaga-Pérez, L.E.; Segura, C.; Bustamante-García, V.; Cápiro, O.G.; Jiménez, R. Torrefaction of wood and bark from Eucalyptus globulus and Eucalyptus nitens: Focus on volatile evolution vs. feasible temperatures. *Energy* **2015**, *93*, 1731–1741. [[CrossRef](#)]
- Bergman, P.C.; Boersma, A.; Zwart, R.; Kiel, J. *Torrefaction for Biomass Co-Firing in Existing Coal-Fired Power Stations*; Energy Research Centre of the Netherlands, ECN-C-05-013; Petten, The Netherlands, 2005.
- Acharya, B.; Dutta, A. Fuel property enhancement of lignocellulosic and nonlignocellulosic biomass through torrefaction. *Biomass Convers. Biorefinery* **2016**, *6*, 139–149. [[CrossRef](#)]
- Nanou, P.; Carbo, M.C.; Kiel, J.H. Detailed mapping of the mass and energy balance of a continuous biomass torrefaction plant. *Biomass Bioenergy* **2016**, *89*, 67–77. [[CrossRef](#)]
- Bach, Q.-V.; Skreiberg, Ø. Upgrading biomass fuels via wet torrefaction: A review and comparison with dry torrefaction. *Renew. Sustain. Energy Rev.* **2016**, *54*, 665–677. [[CrossRef](#)]
- He, C.; Tang, C.; Li, C.; Yuan, J.; Tran, K.-Q.; Bach, Q.-V.; Qiu, R.; Yang, Y. Wet torrefaction of biomass for high quality solid fuel production: A review. *Renew. Sustain. Energy Rev.* **2018**, *91*, 259–271. [[CrossRef](#)]
- Cardona, S.; Gallego, L.J.; Valencia, V.; Martínez, E.; Rios, L.A. Torrefaction of eucalyptus-tree residues: A new method for energy and mass balances of the process with the best torrefaction conditions. *Sustain. Energy Technol. Assess.* **2019**, *31*, 17–24. [[CrossRef](#)]
- Normark, M.; Pommer, L.; Gräsvik, J.; Hedenström, M.; Gorzsás, A.; Winstrand, S.; Jönsson, L.J. Biochemical conversion of torrefied Norway spruce after pretreatment with acid or ionic liquid. *BioEnergy Res.* **2016**, *9*, 355–368. [[CrossRef](#)]
- Sarvaramini, A.; Gravel, O.; Larachi, F. Torrefaction of ionic-liquid impregnated lignocellulosic biomass and its comparison to dry torrefaction. *Fuel* **2013**, *103*, 814–826. [[CrossRef](#)]
- Gomes, P. *A Algarobeira [Prosopis Juliflora]*; Ministério da Agricultura, Pecuária e Abastecimento—MAPA: Brasília, Brazil, 1961.
- Pasiecznik, N.M.; Felker, P.; Harris, P.J.; Harsh, L.; Cruz, G.; Tewari, J.; Cadoret, K.; Maldonado, L.J. *The Prosopis Juliflora-Prosopis Pallida Complex: A Monograph*; HDRA Coventry: Coventry, UK, 2001; Volume 172.

19. Lima, P.C.F. *Manejo de Áreas Individuais de Algaroba: Relatório Final*; EMBRAPA—Brazilian Agricultural Research Corporation: Petrolina, Brazil, 2005; p. 71.
20. Patel, B.; Gami, B.; Bhimani, H. Improved fuel characteristics of cotton stalk, prosopis and sugarcane bagasse through torrefaction. *Energy Sustain. Dev.* **2011**, *15*, 372–375. [[CrossRef](#)]
21. Eseltine, D.; Thanapal, S.S.; Annamalai, K.; Ranjan, D. Torrefaction of woody biomass (Juniper and Mesquite) using inert and non-inert gases. *Fuel* **2013**, *113*, 379–388. [[CrossRef](#)]
22. Natarajan, P.; Suriapparao, D.V.; Vinu, R. Microwave torrefaction of Prosopis juliflora: Experimental and modeling study. *Fuel Process. Technol.* **2018**, *172*, 86–96. [[CrossRef](#)]
23. Basu, P. *Biomass Gasification, Pyrolysis and Torrefaction: Practical Design and Theory*; Elsevier: Amsterdam, The Netherlands, 2018.
24. Dunn, G.; Maier, J.; Scheffknecht, G. Ash fusibility and compositional data of solid recovered fuels. *Fuel* **2010**, *89*, 1534–1540. [[CrossRef](#)]
25. Karampinis, E.; Vamvuka, D.; Sfakiotakis, S.; Grammelis, P.; Itskos, G.; Kakaras, E. Comparative study of combustion properties of five energy crops and Greek lignite. *Energy Fuels* **2012**, *26*, 9. [[CrossRef](#)]
26. Dhyani, V.; Bhaskar, T. A comprehensive review on the pyrolysis of lignocellulosic biomass. *Renew. Energy* **2018**, *129*, 695–716. [[CrossRef](#)]
27. Dhyani, V.; Bhaskar, T. Kinetic analysis of biomass pyrolysis. In *Waste Biorefinery*; Elsevier: Amsterdam, The Netherlands, 2018; pp. 39–83.
28. Doddapaneni, T.R.K.C.; Konttinen, J.; Hukka, T.I.; Moilanen, A. Influence of torrefaction pretreatment on the pyrolysis of Eucalyptus clone: A study on kinetics, reaction mechanism and heat flow. *Ind. Crops Prod.* **2016**, *92*, 244–254. [[CrossRef](#)]
29. Barzegar, R.; Yozgatligil, A.; Olgun, H.; Atimtay, A.T. TGA and kinetic study of different torrefaction conditions of wood biomass under air and oxy-fuel combustion atmospheres. *J. Energy Inst.* **2020**, *93*, 889–898. [[CrossRef](#)]
30. Vyazovkin, S.; Burnham, A.K.; Criado, J.M.; Pérez-Maqueda, L.A.; Popescu, C.; Sbirrazzuoli, N. ICTAC Kinetics Committee recommendations for performing kinetic computations on thermal analysis data. *Thermochim. Acta* **2011**, *520*, 1–19. [[CrossRef](#)]
31. Basu, P.; Rao, S.; Dhungana, A. An investigation into the effect of biomass particle size on its torrefaction. *Can. J. Chem. Eng.* **2013**, *91*, 466–474. [[CrossRef](#)]
32. Yang, H.; Yan, R.; Chen, H.; Zheng, C.; Lee, D.H.; Liang, D.T. In-depth investigation of biomass pyrolysis based on three major components: Hemicellulose, cellulose and lignin. *Energy Fuels* **2006**, *20*, 6. [[CrossRef](#)]
33. Chen, W.-H.; Kuo, P.-C. Isothermal torrefaction kinetics of hemicellulose, cellulose, lignin and xylan using thermogravimetric analysis. *Energy* **2011**, *36*, 6451–6460. [[CrossRef](#)]
34. Saeed, M.A.; Ahmad, S.W.; Kazmi, M.; Mohsin, M.; Feroze, N. Impact of torrefaction technique on the moisture contents, bulk density and calorific value of briquetted biomass. *Pol. J. Chem. Technol.* **2015**, *17*, 23–28. [[CrossRef](#)]
35. Nhuchhen, D.R.; Basu, P.; Acharya, B. A comprehensive review on biomass torrefaction. *Int. J. Renew. Energy Biofuels* **2014**, *2014*, 1–56. [[CrossRef](#)]
36. Aydemir, D.; Gunduz, G.; Ozden, S. The influence of thermal treatment on color response of wood materials. *Color Res. Appl.* **2012**, *37*, 148–153. [[CrossRef](#)]
37. Pelaez-Samaniego, M.R.; Yadama, V.; Lowell, E.; Espinoza-Herrera, R. A review of wood thermal pretreatments to improve wood composite properties. *Wood Sci. Technol.* **2013**, *47*, 1285–1319. [[CrossRef](#)]
38. Chandrasekaran, A.; Ramachandran, S.; Subbiah, S. Determination of kinetic parameters in the pyrolysis operation and thermal behavior of Prosopis juliflora using thermogravimetric analysis. *Bioresour. Technol.* **2017**, *233*, 413–422. [[CrossRef](#)]
39. Suriapparao, D.V.; Pradeep, N.; Vinu, R. Bio-oil production from Prosopis juliflora via microwave pyrolysis. *Energy Fuels* **2015**, *29*, 2571–2581. [[CrossRef](#)]
40. Vassilev, S.V.; Vassileva, C.G.; Vassilev, V.S. Advantages and disadvantages of composition and properties of biomass in comparison with coal: An overview. *Fuel* **2015**, *158*, 330–350. [[CrossRef](#)]
41. Chandrasekaran, A.; Ramachandran, S.; Subbiah, S. Modeling, experimental validation and optimization of Prosopis juliflora fuelwood pyrolysis in fixed-bed tubular reactor. *Bioresour. Technol.* **2018**, *264*, 66–77. [[CrossRef](#)] [[PubMed](#)]
42. Naseeruddin, S.; Yadav, K.S.; Sateesh, L.; Manikyam, A.; Desai, S.; Rao, L.V. Selection of the best chemical pretreatment for lignocellulosic substrate Prosopis juliflora. *Bioresour. Technol.* **2013**, *136*, 542–549. [[CrossRef](#)] [[PubMed](#)]
43. Pereira, J.C.D.; Lima, P.C.F. Comparação da qualidade da madeira de seis espécies de algarobeira para a produção de energia. *Embrapa Semiárido—Artigo em Periódico Indexado* **2002**, *45*, 99–106.
44. Thrän, D.; Witt, J.; Schaubach, K.; Kiel, J.; Carbo, M.; Maier, J.; Ndibe, C.; Koppejan, J.; Alakangas, E.; Majer, S. Moving torrefaction towards market introduction—Technical improvements and economic-environmental assessment along the overall torrefaction supply chain through the SECTOR project. *Biomass Bioenergy* **2016**, *89*, 184–200. [[CrossRef](#)]
45. Chen, W.-H.; Peng, J.; Bi, X.T. A state-of-the-art review of biomass torrefaction, densification and applications. *Renew. Sustain. Energy Rev.* **2015**, *44*, 847–866. [[CrossRef](#)]
46. Bach, Q.-V.; Tran, K.-Q.; Khalil, R.A.; Skreiberg, Ø.; Seisenbaeva, G. Comparative assessment of wet torrefaction. *Energy Fuels* **2013**, *27*, 6743–6753. [[CrossRef](#)]
47. Ho, S.-H.; Zhang, C.; Chen, W.-H.; Shen, Y.; Chang, J.-S. Characterization of biomass waste torrefaction under conventional and microwave heating. *Bioresour. Technol.* **2018**, *264*, 7–16. [[CrossRef](#)] [[PubMed](#)]

48. Wang, S.; Dai, G.; Ru, B.; Zhao, Y.; Wang, X.; Zhou, J.; Luo, Z.; Cen, K. Effects of torrefaction on hemicellulose structural characteristics and pyrolysis behaviors. *Bioresour. Technol.* **2016**, *218*, 1106–1114. [[CrossRef](#)]
49. Neupane, S.; Adhikari, S.; Wang, Z.; Ragauskas, A.J.; Pu, Y. Effect of torrefaction on biomass structure and hydrocarbon production from fast pyrolysis. *Green Chem.* **2015**, *17*, 2406–2417. [[CrossRef](#)]
50. Mei, Y.; Che, Q.; Yang, Q.; Draper, C.; Yang, H.; Zhang, S.; Chen, H. Torrefaction of different parts from a corn stalk and its effect on the characterization of products. *Ind. Crops Prod.* **2016**, *92*, 26–33. [[CrossRef](#)]
51. Hakkou, M.; Pétrissans, M.; Gérardin, P.; Zoulalian, A. Investigations of the reasons for fungal durability of heat-treated beech wood. *Polym. Degrad. Stab.* **2006**, *91*, 393–397. [[CrossRef](#)]
52. Ahmed, M.T.; Hasan, Y.; Islam, S.; Rahman, M. Analysis of Fuel Properties for Peat: A Case Study. *IOSR J. Appl. Chem.* **2019**, *12*, 26–43. [[CrossRef](#)]
53. Lau, H.S.; Ng, H.K.; Gan, S.; Jourabchi, S.A. Torrefaction of oil palm fronds for co-firing in coal power plants. *Energy Procedia* **2018**, *144*, 75–81. [[CrossRef](#)]
54. Ohliger, A.; Förster, M.; Kneer, R. Torrefaction of beechwood: A parametric study including heat of reaction and grindability. *Fuel* **2013**, *104*, 607–613. [[CrossRef](#)]
55. Zhang, Y.; Ashizawa, M.; Kajitani, S.; Miura, K. Proposal of a semi-empirical kinetic model to reconcile with gasification reactivity profiles of biomass chars. *Fuel* **2008**, *87*, 475–481. [[CrossRef](#)]
56. Vamvuka, D.; Kakaras, E. Ash properties and environmental impact of various biomass and coal fuels and their blends. *Fuel Process. Technol.* **2011**, *92*, 570–581. [[CrossRef](#)]
57. Dayton, D.; Jenkins, B.; Turn, S.; Bakker, R.; Williams, R.; Belle-Oudry, D.; Hill, L. Release of inorganic constituents from leached biomass during thermal conversion. *Energy Fuels* **1999**, *13*, 860–870. [[CrossRef](#)]
58. Collard, F.-X.; Blin, J. A review on pyrolysis of biomass constituents: Mechanisms and composition of the products obtained from the conversion of cellulose, hemicelluloses and lignin. *Renew. Sustain. Energy Rev.* **2014**, *38*, 594–608. [[CrossRef](#)]
59. Kan, T.; Strezov, V.; Evans, T.J. Lignocellulosic biomass pyrolysis: A review of product properties and effects of pyrolysis parameters. *Renew. Sustain. Energy Rev.* **2016**, *57*, 1126–1140. [[CrossRef](#)]
60. Mythili, R.; Subramanian, P.; Uma, D. Biofuel production from *Prosopis juliflora* in fluidized bed reactor. *Energy Sources Part A Recovery Util. Environ. Eff.* **2017**, *39*, 741–746. [[CrossRef](#)]
61. Yang, Z.; Zhang, S.; Liu, L.; Li, X.; Chen, H.; Yang, H.; Wang, X. Combustion behaviours of tobacco stem in a thermogravimetric analyser and a pilot-scale fluidized bed reactor. *Bioresour. Technol.* **2012**, *110*, 595–602. [[CrossRef](#)] [[PubMed](#)]
62. Di Blasi, C. Modeling chemical and physical processes of wood and biomass pyrolysis. *Prog. Energy Combust. Sci.* **2008**, *34*, 47–90. [[CrossRef](#)]
63. White, J.E.; Catallo, W.J.; Legendre, B.L. Biomass pyrolysis kinetics: A comparative critical review with relevant agricultural residue case studies. *J. Anal. Appl. Pyrolysis* **2011**, *91*, 1–33. [[CrossRef](#)]
64. Mamvura, T.; Danha, G. Biomass torrefaction as an emerging technology to aid in energy production. *Heliyon* **2020**, *6*, e03531. [[CrossRef](#)]
65. Arteaga-Pérez, L.E.; Grandón, H.; Flores, M.; Segura, C.; Kelley, S.S. Steam torrefaction of *Eucalyptus globulus* for producing black pellets: A pilot-scale experience. *Bioresour. Technol.* **2017**, *238*, 194–204. [[CrossRef](#)] [[PubMed](#)]
66. Sajdak, M.; Kmiec, M.; Micek, B.; Hrabak, J. Determination of the optimal ratio of coal to biomass in the co-firing process: Feed mixture properties. *Int. J. Environ. Sci. Technol.* **2019**, *16*, 2989–3000. [[CrossRef](#)]
67. Grammelis, P.; Skodras, G.; Kakaras, E. Effects of biomass co-firing with coal on ash properties. Part I: Characterisation and PSD. *Fuel* **2006**, *85*, 2310–2315. [[CrossRef](#)]
68. Tumuluru, J.S.; Wright, C.T.; Hess, J.R.; Kenney, K.L. A review of biomass densification systems to develop uniform feedstock commodities for bioenergy application. *Biofuels Bioprod. Biorefining* **2011**, *5*, 683–707. [[CrossRef](#)]